NONEQUILIBRIUM HYDROGEN/NITROGEN PLASMAS STUDIES USING A CASCADE ARC

Trevor Moeller, Dennis Keefer, and Robert Rhodes
University of Tennessee Space Institute
B. H. Goethert Parkway
Tullahoma, TN 37388

ABSTRACT

A cascade arc facility has been constructed at The University of Tennessee Space Institute (UTSI) to study the effect of nonequilibrium transport properties in hydrogen-nitrogen arcjet propellant plasmas. These studies are being used to guide development of the physical models required for further development of arcjet computational codes. The cascade arc has been operated on hydrogen with a current of 50 A at pressures of 2.0 psi and 6.0 psi. Spatially resolved spectral data at these conditions have been collected for the Balmer H_α, H_β, H_γ, and H_δ lines. The experimental H_α lineshapes have been fitted to theoretical, Stark broadened, H_α lineshapes to determine the radial distributions of electron number density. Radial profiles of an equilibrium plasma temperature have also been estimated from Boltzmann plots using the line emission from H_α, H_β, H_γ, and H_δ lines. The electron number densities and plasma temperatures were compared to values predicted by nonequilibrium and equilibrium cascade arc simulations using the UTSI Cascade Arc Plasma Simulation (CAPS) code. The nonequilibrium computer simulations were run using three different sets of finite rate chemical kinetics. By varying finite rate chemical kinetics in the nonequilibrium simulation code, the experimental electric field has been predicted. The nonequilibrium simulations underpredict the peak experimental number densities between 30 percent and 1.5 orders of magnitude. The peak plasma temperature is overpredicted by the simulations by as much as a factor of two. In general, however, the radial profiles of the nonequilibrium solutions better match the experimental measurements.

INTRODUCTION

Electric propulsion thrusters offer significant advantages for satellite station keeping and maneuvering, since their specific impulse can be more than twice that of conventional resistojet or chemical thrusters commonly used for these missions. Computational codes can be used to guide refinements in the configuration of electric propulsion thrusters which lead to better thruster performance, and a number of these codes have been developed for this purpose[1-4]. However, it is now clear that there are important nonequilibrium processes in the propellant plasma which must be understood before adequate physical models can be constructed for use in these computational codes. A cascade arc facility has been constructed at The University of Tennessee Space Institute (UTSI) which permits diagnostic measurements to be made on a controlled nonequilibrium propellant plasma to evaluate the kinetic models and transport properties required for further development of the computational codes.

REASONS FOR UTILIZING A CASCADE ARC RATHER THAN AN ELECTRIC PROPULSION THRUSTER

Some of the most important chemical and transport processes in the propellant plasmas of electric propulsion thrusters, e.g. radial species diffusion and recombination, occur on time scales that are comparable to the convection times in these thrusters. This fast convection produces the strong axial gradients found in the propellant plasma. Therefore, the plasma conditions at a given point in a thruster depend strongly on the previous history of the plasma passing through that point. Comparison of code predictions with measurements in this case requires that the entire upstream flow field be accurately predicted. Differences between measured and predicted quantities could be due to inaccuracies in the models at any point upstream of the measurement location. This makes it very difficult to assess which model mechanisms or rates should be altered to improve the code.

Cascade arcs have long been used as a means to measure the fundamental atomic constants and transport properties of high temperature gases[5]. The cascade arc has a flow velocity much smaller than seen in electric propulsion thrusters, and the length of the arc plasma in the cascade is tens of diameters as compared to one diameter in typical electric propulsion devices. This produces plasmas with properties similar to propellant plasmas in electric propulsion thrusters but with negligible axial gradients. The radial temperature profiles in the cascade arc are controlled primarily by diffusive transport properties rather than convection as seen in electric propulsion thrusters. In the cascade arc, where there are no significant axial gradients, the nonequilibrium plasma parameters are determined by a balance between radial diffusion and chemical reactions and an axially constant but radially dependent energy input. The plasma properties depend on the local conditions at the measurement station rather than a complex time-space convolution of all the conditions upstream of the point of measurement. Differences observed between code predictions and measured quantities are more easily related to the specific reactions or diffusion rates which must be modified to improve the code models.

UTSI EQUILIBRIUM/NONEQUILIBRIUM CASCADE ARC COMPUTER CODE

The equilibrium and nonequilibrium UTSI arcjet computer codes have been modified into one-dimensional nonequilibrium and equilibrium Cascade Arc Plasma Simulation (CAPS) codes[6]. At present these codes model a H_2, H, H^+, e hydrogen system. Both codes include radiation transport. The nonequilibrium version includes species diffusion and a finite rate chemistry kinetics model and uses a two-temperature model with separate energy equations for heavy species and electrons. In both codes it is assumed that the pressure is constant, the radial velocity is zero, and the radial current density is zero. The required mass flow is assured by adjustment of velocity levels. The consequence of these assumptions is that species production and diffusion are locally balanced and total production is balanced by wall losses for the axial momentum, energy, electron energy, and species. The transport properties for both the equilibrium and nonequilibrium versions of the UTSI cascade arc computer code are calculated using a computer code written by Cho based on the procedures developed by DeVoto[7]. The reaction rates for the hydrogen system used in the computer simulations presented in this paper are shown in Table 1. The "slow" and "fast" rates, presented at the 25th AIAA Plasmadynamics and Lasers Conference[2], have different chemical kinetic rates for the three-body ionization and recombination of hydrogen atoms by electrons. The "U of I" (University of Illinois) rates presented at the 26th AIAA Plasmadynamics and Lasers Conference[1] are the same as the "fast" rates but have a different rate for the dissociation of molecular hydrogen by electrons[8]. The forward reaction rates in Table 1 are given by $k_f = a/T^n \exp(E/RT)$. T is the electron temperature for reactions 3, 3 U of I, 5, 5r, and 5i; and M is any third body. Reaction 5r is the slow recombination rate, and 5i is the slow ionization rate.

UTSI CASCADE ARC FACILITY

The UTSI cascade arc is comprised of individually water cooled copper plates separated by electrical insulators (Figure 1). These plates are 3.175 mm (1/8") thick and form a 4 mm diameter arc channel that is approximately 40 mm long. The insulators are ceramic paper or mica 0.254 mm (0.010") thick. A modified plate with windows allows optical access. This section is located in the center of the cascade arc to minimize end effects. The cathode is a 6.35 mm (0.250") diameter thoriated tungsten rod with a 60 degree cone on the end. The anode is 9.144 mm (0.360") diameter thoriated tungsten rod with a blunt end. Both electrodes are cooled by a water jet impinging on their back surface. The arc is driven by a 50 Amp, 600 V power supply. A cascaded centrifugal pump delivers 41.64 liters/min (11 gal/min) of water at 1.38 MPa (200 psi) to cool the copper plates and electrodes. The cascade arc is positioned vertically to eliminate arc asymmetries caused by buoyancy.

Accurate measurement of plasma parameters requires careful integration of the external optics with the design of the central window section. Abel inversion of the emission data is needed to provide radial measurements of the plasma properties[9]. Absolute emission measurements are necessary to determine species concentrations and provide a more accurate measurement of plasma temperatures. To provide a small entrance solid angle for the cascade window section and to avoid off-axis aberrations, an adjustable, reflective Cassegrain optical collection system is used. This collects light from the arc and directs it into a 1.25 meter focal length spectrometer so that the primary mirror in the spectrometer is overfilled. Before entering the Cassegrain telescope the arc image is rotated ninety degrees so that the

radial dimension of the arc image lies along the slit. A two-dimensional optical multichannel analyzer (OMA) with image intensifier is used to collect and digitize the data. This detector has a 512 x 512 pixel detector array with 19 μm pixel spacing and is used to simultaneously acquire spectral data at many radial locations. The magnification of the optical system is approximately 1.0 giving 200 pixels across the 4 mm diameter arc channel. Further details of the experimental setup were presented at the 32nd Joint Propulsion Conference[10].

COMPARISON OF NUMERICAL AND EXPERIMENTAL RESULTS

The cascade arc was operated with pure hydrogen arcs at 2.0 psi and 6.0 psi and a current of 50 A. Spectral emission data from the 656.28 nm Balmer alpha, H_α, line in the 8th order were collected using a 1.25 m Spex spectrometer with a 316 groove/mm echelle grating and a two-dimensional OMA detector[10]. Six images of the arc were collected at each pressure. A 1.9 N.D. filter and a 550 nm high pass filter were utilized to prevent detector saturation and eliminate interference from higher order lines, respectively. The OMA detector exposure times were 0.2 seconds for the 6.0 psi case and 2.0 seconds for the 2.0 psi case. The 2.0 psi case required longer exposure times because the intensity of the radiation was lower for this smaller pressure. The images of the arc have 512 spectral pixels and 400 spatial pixels. Wavelength calibration was performed on the spectral pixels using seven lines from a low density neon calibration source. The spatial pixels were calibrated by taking images of a 50 μm vertical slit backlit by the neon lamp and placed in the same position as the arc when the cascade is in operation. By moving the vertical slit across the location of the arc with a translation table, the spatial pixels were associated with a radial position across the arc region. The spectrometer slit function was spectrally deconvolved from the intensity using a digital Wiener filter[11]. Further details of the experimental procedure were presented at the 32nd Joint Propulsion Conference[10] and the 1st Conference on Synergistic Power and Propulsion Systems Technology[12]. Abel inversion of the spatially resolved line intensity using transform techniques[13] provided spatially resolved emission coefficient line profiles. Electron density was determined by fitting theoretical Stark broadened line profiles[14] to the experimentally measured emission coefficient line profiles. This experiment has been repeated for simulated ammonia and simulated hydrazine at pressures of 2 psi, 6 psi, and 10 psi. Detector exposure times of 2 seconds were used for these measurements.

To obtain estimates of equilibrium plasma temperature distributions in the 50 A hydrogen arcs at 2 psi and 6 psi, emission profiles of the H_α, H_β, H_γ, and H_δ lines were used to make radially resolved Boltzmann plots. The emission profiles were obtained using the Abel inversion technique described above. This data was collected in the second order to guarantee an accurate estimate of the continuum. A standard tungsten filament lamp was used to calibrate the spectral sensitivity of the detector over the range defined by these spectral lines.

RESULTS FOR HYDROGEN PLASMA

Comparisons of the radial distribution of calculated and experimental electron number densities for the 2.0 psi and 6.0 psi cases are presented in Figures 2 and 3, respectively. Results from experiments carried out on two different days are depicted in these figures. The simulations were run using the three sets of finite chemical kinetic rates (Table 1). The error bars on the experimental electron number densities (Figures 2 and 3) are plus or minus one standard deviation of the six realizations at each pressure. At both pressures the nonequilibrium computer simulations underpredict the experimentally determined electron number densities for all radii and for all ionization rates. While the electron number densities are underpredicted by about 1.5 orders of magnitude for the "slow" cases, the results for the "fast" case reduce this underprediction to about a factor of approximately two. The "U of I" case gives the best nonequilibrium solution results; it underpredicts the experimental values by less than an order of magnitude. Like the "U of I" case, the other nonequilibrium distributions have nearly the same profile as the experimental data. The distribution labeled "Ref" is a simulation with "fast" finite rate chemical kinetics and a reflective wall model in which plasma species reflect off of the wall. This case results in more electrons near the wall and predicts the experimental distribution better than the catalytic wall with the same kinetics.

Figure 4 shows a theoretically Stark broadened H_α profile fitted to 6 psi hydrogen arc data at a radius of 1.5 mm. This fit is typical of the those at other

radii. The overprediction of the wings leads to a relatively poor fit, and may be causing the experimental electron number densities to appear larger than they are in reality. Because it is likely that Doppler effects are contributing to the line broadening, the data is better represented by a Voigt profile. Figure 5 shows a Voigt profile fit to the same data in Figure 4. At the writing of this paper, electron number density profiles have not yet been determined using the Voigt line fits, though a significant decrease in the measured electron number densities is anticipated.

Figures 6 and 7 show comparisons of the radial distribution of calculated and experimental temperatures for the 2.0 psi and 6.0 psi cases, respectively. Only the "U of I" nonequilibrium solutions are presented in these plots for the sake of brevity. The computer simulations overpredict the experimental centerline temperatures by approximately 60 percent for the 2.0 psi case and match the experiment (within experimental error) for the 6.0 psi case. The measured temperature profiles do not match any of simulation temperature distributions. The negative temperature gradient at the constrictor wall and the 50 percent error of the experimental temperature distributions make these preliminary data questionable. The error bars on the experimental data are plus or minus one standard deviation calculated from the uncertainty associated with the slope of the line in the Boltzmann plot (the Boltzmann plot of a 6 psi hydrogen arc is shown in Figure 8). The relatively large error in temperature results from poor fits through the four data points in the Boltzmann plots.

Table 2 is a comparison of the experimental and numerical electric field for the 2.0 psi and 6.0 psi cases. The experimental electric fields were determined by finding the slope of the best fit line through the potentials of the cascade plates. The electric fields from the equilibrium simulations overpredict the experimentally determined values by 33 percent for the 2.0 psi case and 10 percent for the 6.0 psi case. These overpredictions increase to 180 percent and 51 percent for the "slow" nonequilibrium simulations at 2.0 psi and 6.0 psi, respectively. The electric field for the "fast" nonequilibrium simulations overpredicts the experiment by 17 percent for 2.0 psi and agrees with the value for 6.0 psi. The "fast" reflective wall solution agrees with the experiment at 2 psi and underpredicts the 6 psi value by 16 percent. The "U of I" nonequilibrium simulations best predict the electric field, splitting the experimental values for the 2.0 psi case and matching the values for the 6.0 psi case. It is evident that the chemical kinetic rates have a large impact on the electric field realized in the nonequilibrium computer simulations.

RESULTS FOR HYDROGEN/NITROGEN PLASMAS

The radial distribution of experimental electron number densities for simulated ammonia and simulated hydrazine are shown in Figures 9 and 10, respectively. These preliminary data show an increase in electron density with pressure, and a very slight increase in electron density for the hydrazine over the ammonia. An interesting feature of the profiles is the positive slope of the curve close to the wall of the arc channel at 2 mm. This feature appears to be the result of relatively poor fits of theoretical Stark line profiles to the noisy data. Filtering of the signal noise for the mixture data has not yet been optimized and may be causing this problem. Table 3 shows a comparison of experimentally determined electric fields for the hydrogen and hydrogen/nitrogen mixtures. The electric field increases with pressure and decreases as more nitrogen is added.

CONCLUSIONS

The predicted hydrogen plasma electron number densities from all of the nonequilibrium computer simulations of the hydrogen cascade arc at 2.0 psi and 6.0 psi underpredict the experimental values by as much as 1.5 orders of magnitude. The peak electron densities are bounded by the equilibrium and the nonequilibrium solutions for the 2.0 psi case, while all of the computer simulations underpredict the peak value for 6.0 psi. Initial fits with Voigt profiles show significant contributions to line broadening that will likely lower the experimental number densities and reduce differences between the experiment and the computer simulations. The experimental electric fields have been bound by nonequilibrium computer simulations using different finite rate chemical kinetics. The "U of I" finite rate chemical kinetics matches the experimental electric field and best predicts the distribution of electron number densities. In addition to obtaining distributions of electron number densities, Boltzmann plots have been used to determine a rough estimate for the

radial distribution of plasma temperature. These preliminary experimental temperature data are overpredicted by the simulations by as much as 2.5 times.

Preliminary electron number density profiles for simulated ammonia and simulated hydrazine have been obtained for 50 Amp arcs at 2 psi, 6 psi, and 10 psi. A hydrogen/nitrogen mixture version of the CAPS code should be available shortly allowing comparisons with the experimental mixture data to commence.

ACKNOWLEDGMENTS

The authors would like to thank Newton Wright, Fred Schwartz, and Nancy O'Brien for their help with the experiment. The authors would also like to thank Dr. L. Montgomery Smith and James Hornkohl for guidance in data analysis. This work was supported by the Air Force Office of Scientific Research under contract #F49620-94-1-0331 and the National Science Foundation under NSF Grant # CTS-9512489.

REFERENCES

1. T. Megli, H. Krier, and R.Burton, "A Plasmadynamics Model for Nonequilibrium Processes in N2/H2 Arcjets," AIAA 95-1961, 26th AIAA Plasmadynamics and Lasers Conference, San Diego, CA, June 19-22, 1995.

2. D. Keefer, D. Burtner, T. Moeller, and R. Rhodes, "Multiplexed Laser Induced Fluorescence and Non-equilibrium Processes in Arcjets," AIAA 94-2656, 25th AIAA Plasmadynamic and Lasers Conference, Colorado Springs, CO, June, 1994.

3. S. Miller, and M. Martinez-Sanchez, "Nonequilibrium Numerical Simulation of Radiation Cooled Arcjets," IEPC-93-218, *Proceedings of the 23rd International Electric Propulsion Conference*, Vol. 3: 2032-2050, Published at The Ohio State University, Columbus OH, 1993.

4. G. W. Butler, B. A .Kashiwa, and D. Q. King, "Numerical Modeling of Arcjet Performance," AIAA 90-1474, AIAA 21st Fluid Dynamics, Plasma Dynamics and Lasers Conference, Seattle, WA, June, 1990.

5. W. L. Wiese, D. R. Paquette, and J. E. Solarski, "Profiles of Stark-Broadened Balmer Lines in a Hydrogen Plasma," *Phys. Rev.*, 129:1225-1232, February, 1963.

6. R. Rhodes, and D. Keefer, "Non-equilibrium Modeling of Hydrogen Arcjet Thrusters," IEPC-93-217, *Proceedings of The 23rd International Electric Propulsion Conference*, Vol. 3: 2020-2031, Published at The Ohio State University, Columbus, OH, 1993.

7. K. Y. Cho, "Non-Equilibrium Thermodynamic Models and Applications to Hydrogen Plasmas," Ph.D. Thesis, Georgia Institute of Technology, March 1988.

8. Janev, et al, Elementary Processes in Hydrogen Helium Plasmas, Springer-Verlag, New York, 1987.

9. H. Griem, *Plasma Spectroscopy*, McGraw-Hill, 1964, pp. 129-167.

10. T. Moeller, D. Keefer, and R. Rhodes, "Cascade Arc Studies of Nonequilibrium Hydrogen Plasmas," AIAA 96-3294, 32nd AIAA/ASME/SAE/ASEE Joint Propulsion Conference, Lake Buena Vista, FL, July 1-3, 1996.

11. R. Gonzalez, and P. Wintz, *Digital Image Processing*, Addison-Wesley Publishing, Ontario, 1977, pp. 199-209.

12. T. Moeller, D. Keefer, and R. Rhodes, " Studies of Nonequilibrium Hydrogen/Nitrogen Plasmas using a Cascade Arc," AIP Conference Proceedings 387, p. 317, The Space Technology and Applications International Forum (STAIF-97), Albuquerque, NM, Jan. 1997.

13. L. M. Smith, D. Keefer, and S.I. Sudharsanan, "Abel Inversion Using Transform Techniques," *J. Quant. Spectrosc. Radiat. Transfer*, 39:367-373, 1988.

14. Griem, H. U., *Spectral Line Broadening by Plasmas,* Academic Press, New York, 1974.

Table 1. Reaction Rates for Hydrogen.

	Reaction	a	n	E
1	$H + H + M \leftrightarrow H_2 + M$	6.40e+17	1.0	0.
2	$H^+ + e + M \leftrightarrow H + M$	5.26e+26	2.5	0.
3 U of I	U of I $H_2 + e \rightarrow H + H + e$	1.87e-3	-3.73	0.
3	$H_2 + e \rightarrow H + H + e$	1.91e+11	-1.0	-203.
4	$H^+ + e \rightarrow H + h\nu$	3.77e+13	0.58	0.
5	fast rates $H^+ + e + e \leftrightarrow H + e$	7.08e+39	4.5	0.
5r	slow rates $H^+ + e + e \rightarrow H + e$	2.19e+41	5.06	0.
5i	$H + e \rightarrow H^+ + e + e$	1.81e+14	0.	-244750

Table 2. Comparison of Experimentally Determined Electric Field (V/cm) with UTSI Cascade Arc Plasma Simulation (CAPS) Code Values.

	Equilibrium Simulation	"Slow" Non-Equilibrium	"Fast" Non-Equilibrium	"Fast" Reflective Wall	"U of I" Non-Equilibrium	Experiment June 20, 1997	Experiment July 16, 1997
Case 1: 2.0 psi	46.4	95.7	42.0	36.4	33.4	36.0 ± 1.2	31.3 ± 1.5
Case 2: 6.o psi	46.3	64.9	43.9	36.9	44.1	44.2 ± 1.2	44.2 ± 1.0

Table 3. Experimentally Determined Electric Field (V/cm) for Hydrogen and Hydrogen/Nitrogen Mixtures.

	Hydrogen July 16, 1997	Simulated Ammonia	Simulated Hydrazine
Case 1: 2.0 psi	31.3 ± 1.5	26.4 ± 0.7	26.2 ± 0.8
Case 2: 6.0 psi	44.2 ± 1.0	38.8 ± 1.1	35.1 ± 0.9

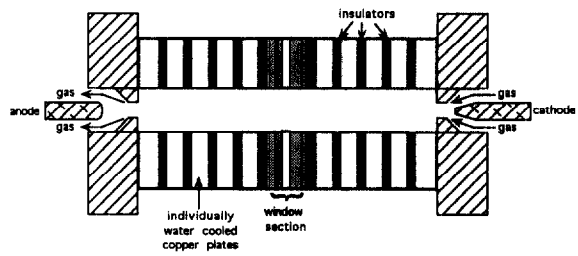

Figure 1. Cascade Arc Assembly.

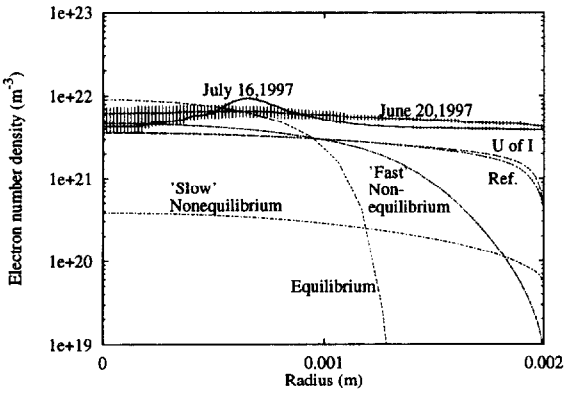

Figure 2. Comparison of Experimental and Numerical Radial Distributions of Electron Number Density in a 50 Amp Hydrogen Arc at 2.0 psi. "Fast" and "slow" represent nonequilibrium computer simulations using two different chemical kinetic rates for the ionization of hydrogen due to electrons. "U of I" indicates a finite rate solution using a different rate for the dissociation of hydrogen by electrons. "Ref" has a reflective wall boundary condition.

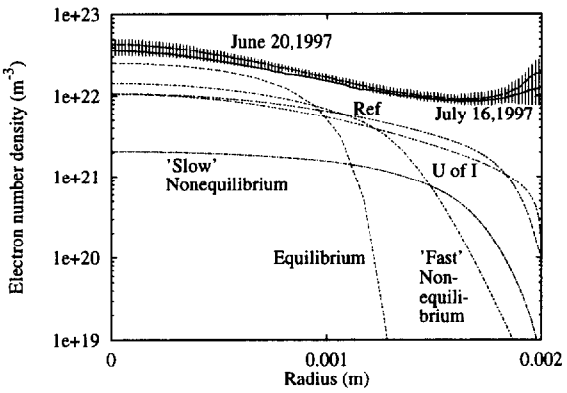

Figure 3. Comparison of Experimental and Numerical Radial Distributions of Electron Number Density in a 50 Amp Hydrogen Arc at 6.0 psi. "Fast" and "slow" represent nonequilibrium computer simulations using two different chemical kinetic rates for the ionization of hydrogen due to electrons. "U of I" indicates a finite rate solution using a different rate for the dissociation of hydrogen by electrons. "Ref" has a reflective wall boundary condition.

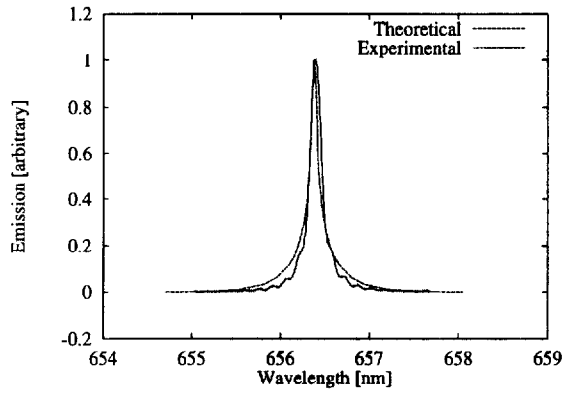

Figure 4. Measured and Fitted Theoretical Stark Lineshapes of H_α Line in a 50 Amp Hydrogen Arc at 6.0 psi at a Radius of 1.5 mm.

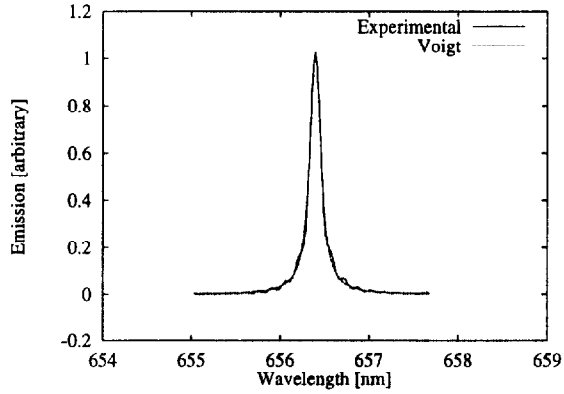

Figure 5. Measured and Fitted Theoretical Voigt Lineshapes of H_α Line in a 50 Amp Hydrogen Arc at 6.0 psi at a Radius of 1.5 mm.

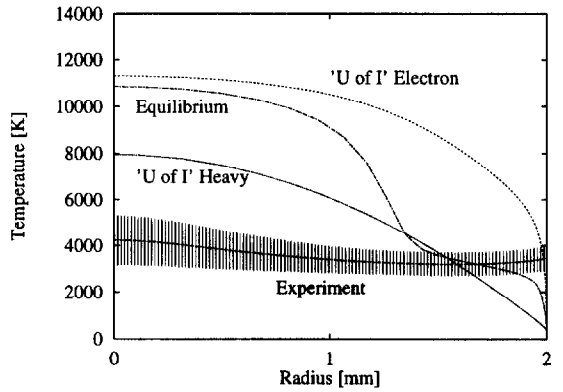

Figure 6. Comparison of Experimental and Numerical Radial Distributions of the Plasma Temperature in a 50 Amp Hydrogen Arc at 2.0 psi. "U of I" indicates a finite rate solution using "U of I" kinetics.

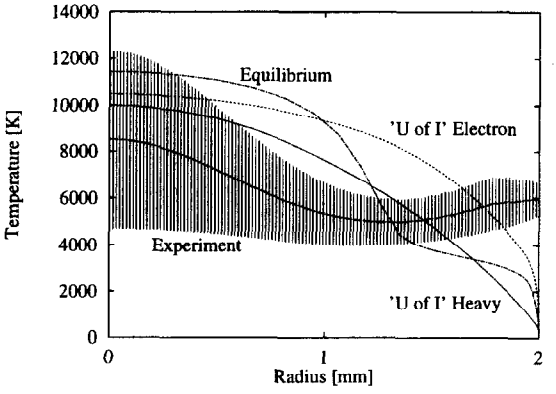

Figure 7. Comparison of Experimental and Numerical Radial Distributions of the Plasma Temperature in a 50 Amp Hydrogen Arc at 6.0 psi. "U of I" indicates a finite rate solution using "U of I" kinetics.

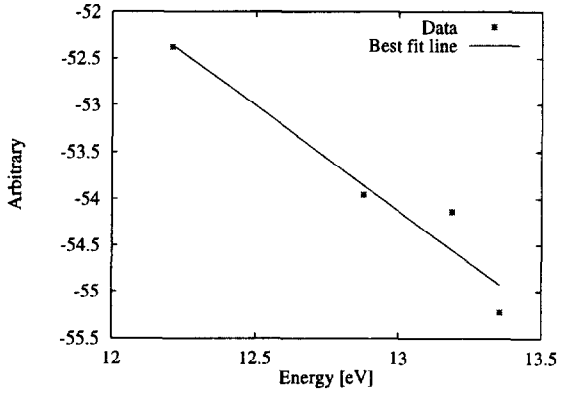

Figure 8. Boltzmann Plot Using the H_α, H_β, H_γ, and H_δ Lines in a 50 Amp Hydrogen Arc at 6.0 psi at a Radius of 1.5 mm.

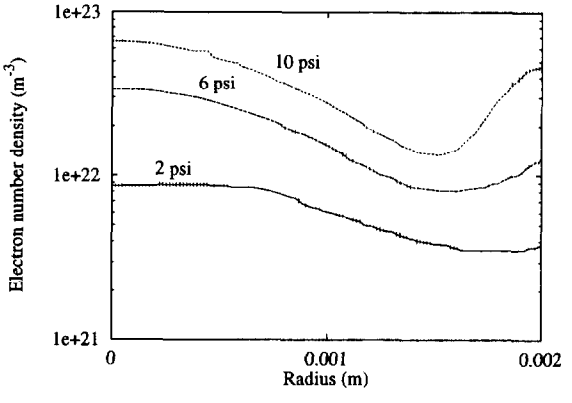

Figure 9. Radial Distributions of Electron Number Densities for Simulated Ammonia (NH_3) at 2.0 psi, 6.0 psi, and 10.0 psi.

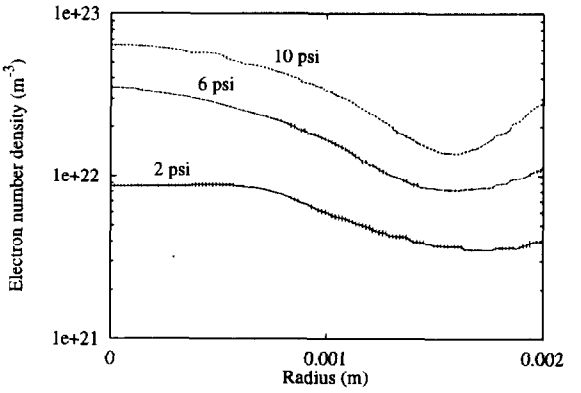

Figure 10. Radial Distributions of Electron Number Densities for Simulated Hydrazine (N_2H_4) at 2.0 psi, 6.0 psi, and 10.0 psi.